Neurobiology of Disease

# Novel Selective Allosteric Activator of the $M_1$ Muscarinic Acetylcholine Receptor Regulates Amyloid Processing and Produces Antipsychotic-Like Activity in Rats

**Carrie K. Jones,[1,5] Ashley E. Brady,[1,5] Albert A. Davis,[8] Zixiu Xiang,[1] Michael Bubser,[3] Mohammed Noor Tantawy,[6] Alexander S. Kane,[1] Thomas M. Bridges,[1] J. Phillip Kennedy,[2] Stefania R. Bradley,[7] Todd E. Peterson,[4,6] M. Sib Ansari,[4,6] Ronald M. Baldwin,[4,6] Robert M. Kessler,[4] Ariel Y. Deutch,[1,3] James J. Lah,[8] Allan I. Levey,[8] Craig W. Lindsley,[1,2,5] and P. Jeffrey Conn[1,5]**

Departments of [1]Pharmacology, [2]Chemistry, [3]Psychiatry, and [4]Radiology and Radiological Sciences/PET Chemistry, [5]Vanderbilt Program in Drug Discovery, and [6]Vanderbilt University Institute of Imaging Science, Vanderbilt University Medical Center, Nashville, Tennessee 37232, [7]ACADIA Pharmaceuticals, San Diego, California 92121, and [8]Center for Neurodegenerative Disease and Department of Neurology, Emory University, Atlanta, Georgia 30322

**Recent studies suggest that subtype-selective activators of $M_1/M_4$ muscarinic acetylcholine receptors (mAChRs) may offer a novel approach for the treatment of psychotic symptoms associated with schizophrenia and Alzheimer's disease. Previously developed muscarinic agonists have provided clinical data in support of this hypothesis, but failed in clinical development because of a lack of true subtype specificity and adverse effects associated with activation of other mAChR subtypes. We now report characterization of a novel highly selective agonist for the $M_1$ receptor with no agonist activity at any of the other mAChR subtypes, termed TBPB [1-(1′-2-methylbenzyl)-1,4′-bipiperidin-4-yl)-1*H*-benzo[*d*]imidazol-2(3*H*)-one]. Mutagenesis and molecular pharmacology studies revealed that TBPB activates $M_1$ through an allosteric site rather than the orthosteric acetylcholine binding site, which is likely critical for its unprecedented selectivity. Whole-cell patch-clamp recordings demonstrated that activation of $M_1$ by TBPB potentiates NMDA receptor currents in hippocampal pyramidal cells but does not alter excitatory or inhibitory synaptic transmission, responses thought to be mediated by $M_2$ and $M_4$. TBPB was efficacious in models predictive of antipsychotic-like activity in rats at doses that did not produce catalepsy or peripheral adverse effects of other mAChR agonists. Finally, TBPB had effects on the processing of the amyloid precursor protein toward the non-amyloidogenic pathway and decreased A$\beta$ production *in vitro*. Together, these data suggest that selective activation of $M_1$ may provide a novel approach for the treatment of symptoms associated with schizophrenia and Alzheimer's disease.**

*Key words:* **TBPB; $M_1$ allosteric agonist; muscarinic acetylcholine receptors; schizophrenia; Alzheimer's disease; mAChR**

## Introduction

Muscarinic acetylcholine receptors (mAChRs) modulate multiple functions of the CNS, including cognition and motor control. The mAChRs are members of the family A G-protein-coupled receptors (GPCRs) and include five subtypes, termed $M_1$–$M_5$ (Bonner et al., 1987, 1988). With the broad diversity of functions of mAChRs, development of subtype-selective mAChR ligands has the potential to provide novel therapeutic approaches for multiple disease states, including symptoms associated with schizophrenia and Alzheimer's disease (AD).

Previous studies suggest that selective activation of mAChRs may reduce psychotic symptoms and cognitive impairments in individuals suffering from AD and schizophrenia. For example, the $M_1/M_4$-preferring mAChR agonist xanomeline produced a robust reduction in behavioral disturbances in individuals with AD (Bodick et al., 1997a,b) and the positive and negative symptoms in schizophrenic patients (Shekhar et al., 2008). Xanomeline also has robust efficacy in a number of animal models predictive of antipsychotic activity (Shannon et al., 2000; Perry et al., 2001). Unfortunately, the clinical effects of xanomeline and other muscarinic agents are associated with adverse side effects attributable to nonspecific activation of peripheral $M_2$ and $M_3$ mAChRs, including gastrointestinal distress, bradycardia, and salivation (Bymaster et al., 1998). At present, the relative contributions of $M_1$ and $M_4$ mAChRs to the clinical effects of xanomeline or effects in associated animal models remain unknown.

Previous attempts to develop highly selective agonists of $M_1$ have likely failed because of the high sequence conservation of the

Received April 27, 2008; revised July 20, 2008; accepted July 30, 2008.

This work was supported by grants from the National Institute of Mental Health (P.J.C., C.K.J., A.E.B.), the National Institute of Neurological Disorders and Stroke (A.I.L.), and Alzheimer's Association Grant IIRG-07-57131 (C.W.L.), a predoctoral fellowship from the National Institute on Aging and the PhRMA Foundation (A.A.D.), the Dystonia Medical Research Foundation Grant (Z.X.), and Career Award at the Scientific Interface from the Burroughs Wellcome Fund (T.E.P.).Vanderbilt is a site in the National Institutes of Health-supported Molecular Libraries Screening Center Network. Parts of this work have been presented previously at the 45th Annual Meeting of the American College of Neuropsychopharmacology, Hollywood, Florida, December 3–7, 2006.

Correspondence should be addressed to Dr. P. Jeffrey Conn, Director, Vanderbilt Program in Drug Discovery, Department of Pharmacology, Vanderbilt University Medical Center, 2220 Pierce Avenue, 1215 Light Hall, Nashville, TN 37232-6600. E-mail: jeff.conn@vanderbilt.edu.

DOI:10.1523/JNEUROSCI.1850-08.2008

 0270-6474/08/2810422-12$15.00/0

orthosteric binding site of the mAChRs. An alternate approach to orthosteric muscarinic agonists is targeting allosteric sites to activate the receptor by actions at a site removed from the highly conserved acetylcholine (ACh) binding site. In recent years, we (Rodriguez et al., 2005; Hemstapat et al., 2007; Shirey et al., 2008) and others (for review, see Christopoulos, 2002; Waelbroeck et al., 2003) have successfully developed allosteric modulators of a number of GPCRs that provide unprecedented selectivity for the intended receptor. Recently, Spalding et al. (2002, 2006) identified AC42 [4-(4-butylpiperidin-1-yl)-1-o-tolylbutan-1-one] as a selective allosteric agonist at the $M_1$ receptor. However, AC42 and analogs have limited potency and pharmacokinetic properties unsuitable for use *in vivo*.

We have characterized a novel series of selective allosteric agonists for the $M_1$ receptor, represented by TBPB [1-(1′-2-methylbenzyl)-1,4′-bipiperidin-4-yl)-1*H* benzo[*d*]imidazol-2(3*H*)-one] (Jones et al., 2006; Kinney et al., 2006), which is structurally unrelated to any previously reported orthosteric or allosteric mAChR agonists. We now report that TBPB is a highly selective, allosteric agonist of $M_1$ with no agonist activity at the other mAChR subtypes. TBPB selectively potentiates the NMDA subtype of glutamate receptor (NMDAR) currents in hippocampal pyramidal cells. Interestingly, TBPB has similar effects as less selective mAChR agonists on amyloid processing in PC12 cells. Furthermore, TBPB has robust effects in animal models predictive of antipsychotic-like activity that are similar to those reported previously for xanomeline or atypical antipsychotics. Together with previous clinical studies, these data raise the exciting possibility that highly selective allosteric agonists of $M_1$ may provide a novel therapeutic approach for the treatment of symptoms associated with schizophrenia and AD.

## Materials and Methods

### Cell culture and transfections

Chinese hamster ovary (CHO-K1) cells stably expressing rat (r) $M_1$ were purchased from the American Type Culture Collection and cultured according to their suggested protocol. CHO cells stably expressing human (h) $M_2$, $hM_3$, and $hM_5$ were used and described previously (Levey et al., 1991); $rM_4$ cDNA, provided by T. I. Bonner (National Institutes of Health, Bethesda, MD), was used to stably transfect CHO-K1 cells purchased from the American Type Culture Collection using Lipofectamine 2000. To make stable $hM_2$ and $rM_4$ cell lines for use in calcium mobilization assays, these cells also were stably transfected with a chimeric G-protein ($G_{qi5}$) using Lipofectamine 2000. $rM_1$, $hM_3$, and $hM_5$ cells were grown in Ham's F-12 medium containing 10% heat-inactivated fetal bovine serum (FBS), 2 mM GlutaMax I, 20 mM HEPES, and 50 μg/ml G418 sulfate. $hM_2$–$G_{qi5}$ cells were grown in the same medium also containing 500 μg/ml Hygromycin B. Stable $rM_4$–$G_{qi5}$ cells were grown in DMEM containing 10% heat-inactivated FBS, 2 mM GlutaMax I, 1 mM sodium pyruvate, 0.1 mM nonessential amino acids, 20 mM HEPES, 400 μg/ml G418 sulfate, and 500 μg/ml Hygromycin B. The rat $M_1$ Y381A orthosteric mutant receptor cDNA was generated using the QuickChange site-directed mutagenesis kit (Stratagene) and verified by sequencing. CHO-K1 cells were stably transfected with this cDNA using Lipofectamine 2000 and screened for expression based on calcium mobilization in response to the allosteric $M_1$ agonist *N*-desmethylclozapine.

### Calcium mobilization assays

For measurement of agonist-evoked increases in intracellular calcium, CHO-K1 cells stably expressing muscarinic receptors were plated in 20 μl of growth medium lacking antibiotic at $1 \times 10^4$ ($rM_1$, $hM_3$, and $hM_5$) or $2.5 \times 10^4$ cells per well ($rM_1$ Y381A, $hM_2$, and $rM_4$) in Greiner 384-well black-walled, tissue culture (TC)-treated, clear-bottom plates (VWR). Cells were grown overnight at 37°C and 5% $CO_2$. The next day, medium was removed from the cells, and they were incubated with 20 μl of 2 μM Fluo-4 AM diluted in assay buffer [HBSS (Invitrogen) supplemented with 20 mM HEPES and 2.5 mM probenecid, pH 7.4] for 1 h at 37°C. Dye was removed and replaced with 40 μl of assay buffer. Agonists were diluted into assay buffer at a 5× concentration and applied to cells using the automated system at 11 s into the 120 s protocol. Calcium flux was measured over time as an increase in fluorescence (fold over basal) using the Hamamatsu Functional Drug Screening System (FDSS-6000). Data were collected at 1 Hz.

### Schild analysis

Schild analyses were performed at 25°C on a FLEXstation II (Molecular Devices) by measuring calcium mobilization in response to agonist [carbachol (CCh) or TBPB] stimulation in the presence of various fixed concentrations of the antagonist atropine. CHO-K1 cells stably expressing $rM_1$ were plated at $5 \times 10^4$ cells per well in 100 μl growth medium in Costar 96-well cell culture plates (Corning). The next day, cells were loaded with 2 μM calcium indicator dye Fluo-4 AM (Invitrogen) for 45 min at 37°C. Dye was removed and replaced with 45 μl of assay buffer, pH 7.4 (1× HBSS, supplemented with 20 mM HEPES and 2.5 mM probenecid). Immediately after dye loading, cells were preincubated for 15 min with 45 μl of varying fixed concentrations of atropine prepared at a 2× concentration before placing the assay plate in the Flexstation II for agonist addition. Agonist concentration–response curves were prepared in assay buffer at a 10× concentration. The Flexstation II was programmed to add 10 μl of 10× agonist at 19 s into the 45 s protocol, with data being read every 1.52 s (excitation at 488 nm/emission at 525 nm). The signal amplitude was first normalized to baseline and then expressed as a percentage of the maximal response to acetylcholine.

### Amyloid precursor protein and amyloid-β assays

#### *Cell culture and drug treatments*

PC12 N21 cells (a gift from Dr. Richard Burry, Ohio State University, Columbus, OH) were maintained in DMEM containing 10% horse serum, 5% fetal clone, 100 U/ml penicillin, and 100 μg/ml streptomycin at 37°C and 5% $CO_2$. For amyloid processing experiments, cells were plated at 50,000 cells/$cm^2$ in 60 mm culture dishes 4 d before the experiment. On the day of the experiment, the medium was replaced with 1.5 ml serum-free DMEM containing the vehicle [dimethylsulfoxide (DMSO)] or the indicated drugs. Cells were incubated at 37°C for 8 h, after which 1 ml of conditioned medium was collected and centrifuged at 17,000 × *g* for 5 min to remove any cellular debris. Cells were placed on ice, rinsed with cold PBS, and harvested in PBS containing protease inhibitor cocktail (Roche Diagnostics).

#### *Lentivirus transduction*

A humanized amyloid precursor protein sequence bearing the Swedish mutation (KM670/671/NL) was cloned in place of green fluorescent protein (GFP) in the FUGW backbone. High titer virus (~$1 \times 10^9$ infectious particles/ml) was used to transduce PC12 N21 cells. The amyloid precursor protein (APP)-infected cells were subsequently infected with a lentivirus in which GFP was replaced by the human $M_1$ muscarinic receptor sequence.

#### *Amyloid-β ELISA*

Amyloid-$\beta_{40}$ ($A\beta_{40}$) levels were measured using the hAmyloid β40 ELISA (HS) kit (The Genetics Company) according to the instructions of the manufacturer. Plates were read at 450 nm on a Spectra Max Plus plate reader (Molecular Devices).

#### *Antibodies*

Primary antibodies included 6E10 (APP Aβ domain; Signet) and C8 (APP C terminus; a gift from Dr. Dennis Selkoe, Center for Neurologic Diseases, Harvard Medical School, Boston, MA).

#### *Western blotting*

A total of 50 μg of protein from cell extracts or 15 μl of conditioned medium was prepared in Laemmli's sample buffer, separated by SDS-PAGE, and transferred to Immobilon-P membranes (Millipore, Bedford, MA). Membranes were blocked at room temperature for 30 min and incubated with primary antibodies overnight at 4°C. Blots were rinsed

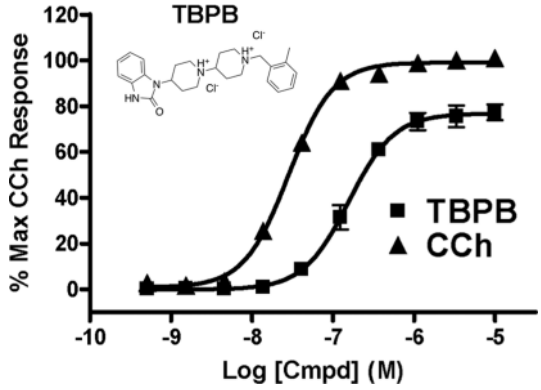


**Figure 1.** TBPB is an allosteric agonist of $M_1$ receptors in recombinant systems. TBPB (■; $EC_{50}$ of 158 ± 21 nM) and carbachol (▲; $EC_{50}$ of 28.6 ± 2.2 nM) elicit a robust response in CHO-K1 cells expressing WT $rM_1$. Data are mean ± SEM of three to six independent experiments each performed in quadruplicate.

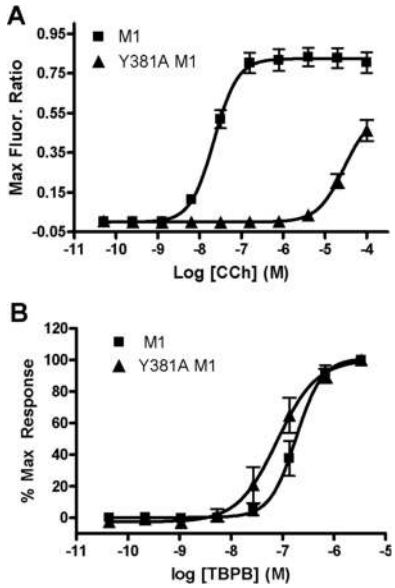


**Figure 2.** TBPB activity is consistent with action as an allosteric agonist *in vitro*. ***A***, The Y381A mutation robustly shifts the $M_1$ response to CCh. WT $rM_1$ (■) $EC_{50}$ of 23.2 ± 2.2 nM. ***B***, TBPB activates the Y381A mutant with an $EC_{50}$ similar to the WT $rM_1$. $rM_1$ (■) $EC_{50}$ of 220 ± 62 nM; Y381A (▲) $EC_{50}$ of 97.7 ± 36 nM. Data are mean ± SEM of five to six independent experiments each performed in quadruplicate.

and incubated with fluorophore-conjugated secondary antibodies (Invitrogen and Rockland) for 1 h at room temperature. Blots were imaged, and band intensities were quantified using an Odyssey Image Station (LI-COR).

## Hippocampal slice electrophysiology

Transverse hippocampal slices were prepared from Sprague Dawley rats (postnatal days 21–25). In brief, rats were anesthetized with isoflurane and decapitated. The brain was rapidly removed from the skull and submerged in ice-cold modified artificial CSF (ACSF), which was oxygenated with 95% $O_2$/5% $CO_2$ and composed of the following (in mM): 230 sucrose, 2.5 KCl, 0.5 $CaCl_2$, 10 $MgSO_4$, 1.25 $NaH_2PO_4$, 26 $NaHCO_3$, and 10 D-glucose. The brain was then blocked in the horizontal plane, glued to the stage of a vibratome (Vibratome) that was filled with ice-cold modified ACSF, and cut at a thickness of 290 μm. Slices were then incubated in oxygenated normal ACSF (in mM: 126 NaCl, 2.5 KCl, 3 $CaCl_2$, 1 $MgSO_4$, 1.25 $NaH_2PO_4$, 26 $NaHCO_3$, and 10 D-glucose) at 31–32°C for 1 h and then maintained at room temperature until being transferred individually to a fully submerged recording chamber, which was continuously perfused with oxygenated ACSF at ~30°C.

Whole-cell recordings were made from visually identified hippocampal CA1 pyramidal neuron soma under an Olympus BX50WI upright microscope. A low-power objective (4×) was used to identify CA1 region of the hippocampus, and a 40× water immersion objective coupled with Hoffman optics and video system was used to visualize individual pyramidal cells. A MultiClamp amplifier (Molecular Devices) was used for voltage-clamp recordings. Patch pipettes (3–5 MΩ) were prepared from borosilicate glass (World Precision Instrument) using a Narashige vertical patch pipette puller and filled with the pipette solution containing the following (in mM): 61.5 K-gluconate, 65 CsCl, 3.5 KCl, 1 $MgCl_2$, 0.5 $CaCl_2$, 10 HEPES, 5 EGTA, 2 Mg-ATP, and 0.2 Na-GTP. The pH of the pipette solution was adjusted to 7.3 with 1 M KOH, and osmolarity was adjusted to ~295 mOsm. NMDA receptor-mediated currents were induced by pressure ejection of 0.5 mM NMDA to the soma of the recorded cell using a Picospritzer II (General Valve). This experiment was performed in the presence of tetrodotoxin (1 μM) to block voltage-gated sodium channels, and the cell was typically voltage clamped at −60 mV. EPSCs or IPSCs were evoked in CA1 pyramidal cells by electrical stimulation of Schaffer collaterals using a concentric bipolar stimulating electrode (FHC) in the presence of the $GABA_A$ receptor antagonist bicuculline (20 μM) or ionotropic glutamate receptor antagonists CNQX (10 μM) and AP-5 (50 μM), respectively. In these experiments, cells were typically voltage clamped at −60 to −70 mV. All drugs were bath applied. Data analysis was performed using a personal computer equipped with pClamp data acquisition and analysis software (Molecular Devices). Data were presented as percentage of the control value or percentage potentiation. The percentage potentiation was defined by $[I_{max}/I_{control} - 1] \times 100$, where $I_{control}$ was the average amplitude of NMDA receptor currents of four trials immediately before application of TBPB, and $I_{max}$ is the maximum current amplitude during TBPB application. TBPB was dissolved in DMSO and then diluted to the appropriate concentration using ACSF.

## Fos immunohistochemistry

Two hours after drug treatment, rats were deeply anesthetized with isoflurane and transcardially perfused with PBS followed by 4% paraformaldehyde. Brains were postfixed overnight and cryoprotected in 30% sucrose, and coronal sections through the forebrain were cut at 42 μm on a freezing microtome. For the demonstration of Fos-like immunoreactivity (Fos-li), free-floating sections were incubated in a goat anti-Fos antibody (1:3000; Santa Cruz Biotechnology) and processed following our previously described methods (Young et al., 1999; Bubser et al., 2002).

## Amphetamine-induced hyperlocomotion

*Subjects.* All behavioral studies were conducted using male Harlan Sprague Dawley rats, weighing 275–300 g. Subjects were housed in groups in a large colony room under a 12 h light/dark cycle (lights on at 6:00 A.M.) with food and water provided *ad libitum*. Test sessions were performed between 6:00 A.M. and 6:00 P.M. All dose groups consisted of 6–12 rats. All experiments were conducted in accordance with the National Institutes of Health regulations of animal care covered in *Principles of Laboratory Animal Care* (National Institutes of Health publication 85-23, revised 1985) and were approved by the Institutional Animal Care and Use Committee.

*Apparatus.* Amphetamine-induced hyperlocomotion studies were conducted in open-field chambers (27 × 27 × 20 cm) (Hamilton Kinder) equipped with 16 horizontal (*x*- and *y*-axes) infrared photobeams. Changes in locomotor activity were measured as the number of photobeam breaks and were recorded with a Pentium I computer equipped with mouse activity monitoring system software (Hamilton Kinder).

*Procedure.* Male Harlan Sprague Dawley rats were habituated in locomotor activity test chambers for 30 min and then injected subcutaneously with vehicle or a dose of TBPB. At 60 min, all rats were injected subcutaneously with 1 mg/kg amphetamine and then tested for an additional 60 min. Data are expressed as changes in ambulation, total number

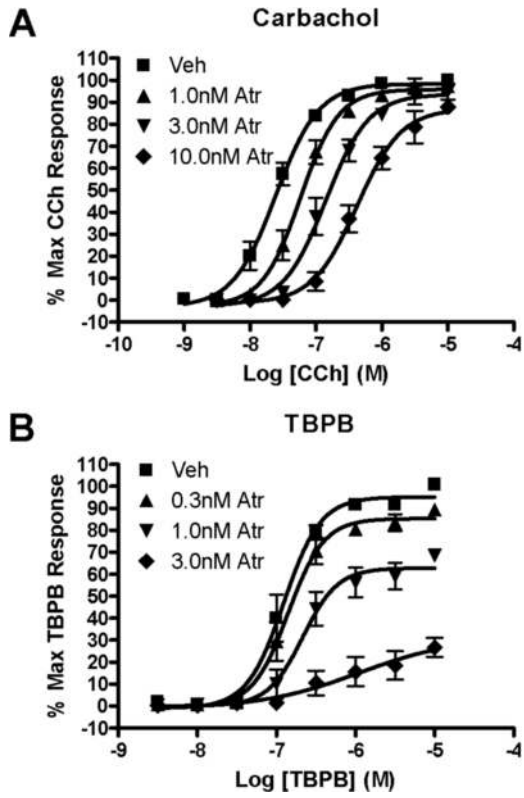


**Figure 3.** Atropine noncompetitively antagonizes TBPB at $M_1$. ***A***, Increasing concentrations of atropine (Atr) (1–10 nM) competitively antagonize the action of CCh at the $rM_1$. ***B***, Increasing concentrations of atropine (0.3–3.0 nM) produced a concentration-dependent decrease in the maximum effect of TBPB in CHO-K1 cells expressing WT $rM_1$. Data are mean ± SEM of three to six independent experiments each performed in triplicate. Veh, Vehicle.

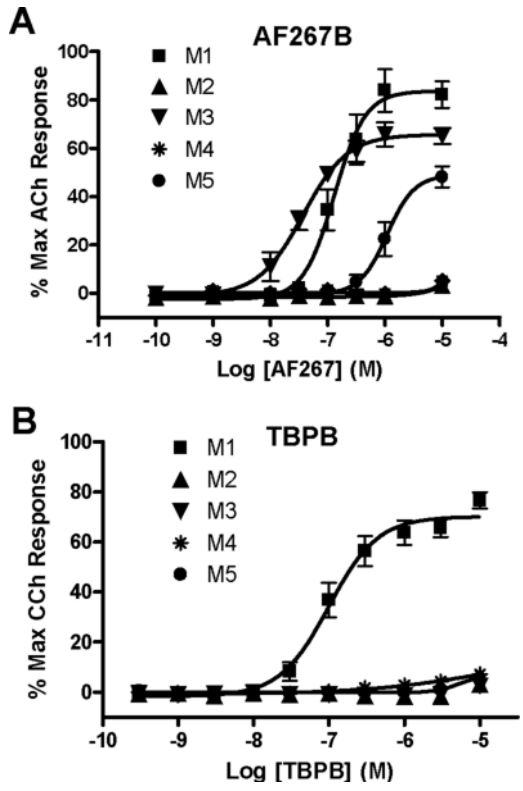


**Figure 4.** TBPB is a highly selective agonist for the $M_1$ receptor. ***A***, Concentration–response curves for the orthosteric agonist AF267B across the $M_1$–$M_5$ mAChRs. $rM_1$ $EC_{50}$ of 149.7 nM (84.2% ACh Max), $hM_2$ $EC_{50} > 50$ μM, $hM_3$ $EC_{50}$ of 38.2 nM (75.5% ACh Max), $rM_4$ $EC_{50} > 50$ μM, $hM_5$ $EC_{50}$ of 1.08 μM (48.5% ACh Max). ***B***, TBPB selectively activates the $rM_1$ subtype of muscarinic acetylcholine receptor. $rM_1$ (■) $EC_{50}$ of 112 ± 3.1 nM. Data are mean ± SEM of three independent experiments each performed in quadruplicate.

of beam breaks per 5 min bins. Each point represents the mean value for 8–12 rats per dose group. The vertical lines represent ±SEM values.

In a separate experiment, the effects of TBPB (30, 56.6, and 100 mg/kg, s.c.) on locomotor activity when administered alone were assessed in nonhabituated naive rats. In this experiment, rats were pretreated with vehicle or dose of TBPB for 30 min and then placed into the open-field chambers, and changes in locomotor activity were assessed for 60 min. Data are expressed as changes in ambulation, total number of beam breaks per 5 min bins. Each point represents the mean value for 8–12 rats per dose group. The vertical lines represent ±SEM values.

### Catalepsy test

Male Harlan Sprague Dawley rats were injected subcutaneously with vehicle or a dose of TBPB, haloperidol, or clozapine and then tested at time points for up to 4 h in catalepsy test. Catalepsy was evaluated by placing both forepaws on a horizontal rod 6 cm above the bench top and recording the time until the rat returned both forepaws to the floor of the test cage (Moore et al., 1992). The data are expressed as the immobility time, i.e., the number of seconds until the rats returned both feet to the floor of the test cage. Each point represents the mean value for six rats per dose group.

### Modified Irwin test battery procedure

Changes in the Modified Irwin Neurological Battery as reported previously (Irwin, 1968) were evaluated using a rating scale from 0 to 2: 0, no effect; 1, modest effects; 2, robust effect. All rats were pretreated with vehicle, a dose of oxotremorine (0.03–0.3 mg/kg, s.c.), or TBPB (30–100 mg/kg, s.c.) and then tested in the Irwin battery at 30 min after treatment.

### $D_2$ occupancy studies using positron emission tomography

Male Sprague Dawley rats, weighing 275–300 g, were habituated for 5 min in a rat tail veining restraint cylinder for 3 consecutive days, before the first and second days of testing. On the first day, rats were injected with vehicle subcutaneously 30 min before a tail-vein injection of ~350 μCi (range, 250–450 μCi) of [$^{18}$F]fallypride [(*S*)-*N*-[(1-allyl-2-pyrrolidinyl)methyl]-5-(3′-[$^{18}$F]fluoropropyl)-2,3-dimethoxybenzamide] using a catheter. The catheter was then removed and measured for residual activity. After injection, rats were returned to their cages for a 60 min [$^{18}$F]fallypride uptake period with access to food and water *ad libitum*. Rats were then anesthetized under 1.5% isoflurane and imaged for 60 min (Tantawy et al., 2007) in the microPET Focus 220 (Siemens). One week later, the same rats were pretreated with a dose of TBPB (100 mg/kg, s.c.) 30 min before or with haloperidol (0.1 or 1.0 mg/kg, s.c.) 60 min before injection with [$^{18}$F]fallypride. After 60 min, rats were anesthetized under 1.5% isoflurane and imaged for 60 min in the microPET. Scatter and attenuation corrections were applied for all microPET scans for all groups. Attenuation maps for these corrections were created from a transmission image acquired using a $^{57}$Co source. The data were reconstructed on a 128 × 128 × 95 grid at a pixel size of 0.095 cm and slice thickness of 0.080 cm. Dynamic images were reconstructed using an OSEM2D algorithm with a sequence of five 60 s frames (5 × 60 s), 2 × 300 s, 2 × 600 s, 2 × 1200 s, 1 × 600 s, 6 × 300 s, 2 × 600 s, and 3 × 1200 s. Three dimensional regions of interest (ROIs) were drawn around the cerebellum, left striatum (STR), and right STR using AsiPro software. Time–activity curves from these ROIs were used as input to the Logan plot analysis from which estimates of binding potential were obtained.

### Statistical analysis

For the calcium mobilization assay, all data were normalized to percentage CCh or TBPB maximum defined by 10 μM CCh or TBPB for each cell line, respectively. Data analysis was performed using Prism 4.0 software (GraphPad Software). For the Fos immunoreactivity studies, Fos-li cells were charted, and their density was quantified using NeuroLucida soft-

ware (MicroBrightField). Fos expression was analyzed in the prelimbic area of the prefrontal cortex (PFC) (in a column extending from pial surface to forceps minor) and in a box (200 × 300 μm) placed in the medial and lateral striatum and core and shell subregions of the nucleus accumbens (NAS). All data are presented as means ± SEM of the number of Fos-li neurons per square millimeter. Behavioral data were analyzed by using a one-way ANOVA with treatment as the main factor. When a statistically significant effect was found, *post hoc* analysis was performed by using a Dunnett's test. Electrophysiological, Fos, and positron emission tomography (PET) data were analyzed by using a one- or two-tailed Student's *t* test. For the PET studies, changes in binding potential (BP) of [$^{18}$F]fallypride for $D_2$ in rat striatum (caudate–putamen), a region with high $D_2$ dopamine receptor expression levels, were calculated from distribution volume ratio (DVR) estimates (DVR = BP + 1) using a Logan plot reference tissue model with the cerebellum as the reference region. Percentage $D_2$ dopamine receptor occupancy was calculated as (1 − [binding potential$_{drug}$/binding potential$_{control}$]) × 100.

### Chemicals

ACh, carbamylcholine chloride (carbachol), probenecid, and DMSO were purchased from Sigma-Aldrich. Fluo-4 AM calcium-sensitive dye and all tissue culture reagents were purchased from Invitrogen. Greiner optical bottom TC-treated 384-well culture plates were obtained from VWR. [$^{18}$F]Fallypride synthesis was performed in the computer-controlled processor unit of the CTI RDS-112 cyclotron prepared using modifications of our previously reported methods (Kessler, 1993; Ansari, 2006) in specific activities of > 2000 Ci/mmol. Fluorine-18 radioactivity was counted in a Capintec dose calibrator, and low-level counting was performed in a well counter (Auto-Gamma 5000; PerkinElmer Life and Analytical Sciences). Autoradiograms were read and analyzed using the Cyclone Storage Phosphor System (PerkinElmer Life and Analytical Sciences). Amphetamine hydrochloride, oxotremorine sesquifumarate, haloperidol (Sigma-Aldrich), and TBPB (synthesized in-house by the Lindsley laboratory) were used.

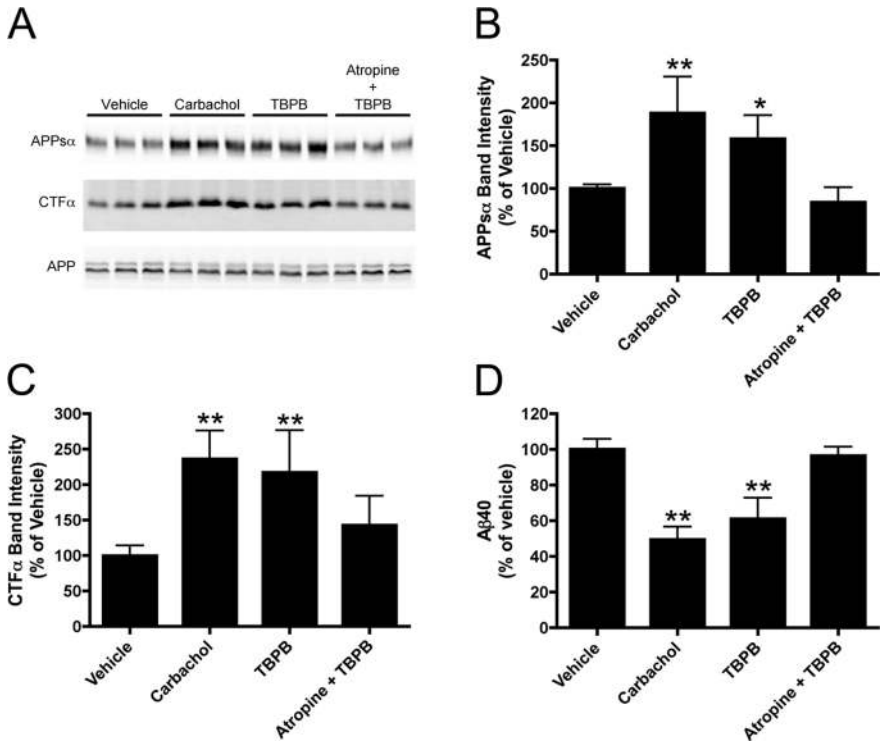


**Figure 5.** TBPB regulates non-amyloidogenic APP processing. ***A***, Western blots of conditioned media and cell lysates demonstrate increased production of $APP_{s\alpha}$ and CTF$\alpha$ in cells treated with CCh and TBPB. ***B***, Quantitation of $APP_{s\alpha}$ band intensity shows a significant increase in $APP_{s\alpha}$ shedding from CCh- and TBPB-treated cells (*$p < 0.01$, $n = 7$ across 3 separate experiments for TBPB; **$p < 0.001$, $n = 7$ across 3 separate experiments for CCh). ***C***, Quantitation of CTF$\alpha$ band intensity demonstrates a significant increase in production of CTF$\alpha$ in CCh- and TBPB-treated cells (**$p < 0.001$, $n = 16$ across 6 separate experiments). ***D***, ELISA measurements from conditioned media show a significant decrease in secreted A$\beta_{40}$ from cells treated with either CCh or TBPB (**$p < 0.001$, $n = 6$ across 2 separate experiments for CCh; **$p < 0.001$, $n = 9$ across 3 separate experiments for TBPB).

## Results

### TBPB is a selective, allosteric agonist of the $M_1$ receptor in recombinant systems

Activation of $M_1$ was assessed by measuring agonist-induced increases in intracellular calcium in CHO-K1 cells expressing wild-type (WT) rat $M_1$ with a functional fluorescence-based calcium assay. Both the orthosteric agonist CCh and TBPB produced robust increases in intracellular calcium in cells expressing WT $rM_1$ (Fig. 1). The response to TBPB was 77.3 ± 3.4% of the maximal response to CCh with an $EC_{50}$ of 158 ± 21 nM. The response to TBPB was not observed in untransfected parental CHO-K1 cells and was blocked by the mAChR antagonist atropine (data not shown), demonstrating that this is an $M_1$-mediated response.

Allosteric agonists of $M_1$ can be differentiated from orthosteric agonists by their ability to activate a form of the receptor in which there is a single point mutation in the orthosteric site that renders the receptor insensitive to acetylcholine or orthosteric agonists (Spalding et al., 2002, 2006; Jones et al., 2006; Kinney et al., 2006). To determine whether TBPB is likely acting as an allosteric agonist of $M_1$, we evaluated the effects of TBPB in a cell line stably expressing $rM_1$ receptor containing this mutation (tyrosine 381 to alanine; Y381A) in the orthosteric binding site. CCh was without effect at $rM_1$ Y381A at concentrations that fully activated the WT $rM_1$ receptor (Fig. 2*A*). In contrast, increasing concentrations of TBPB activated the $rM_1$ Y381A mAChR mutant with an $EC_{50}$ similar to the WT $rM_1$ mAChR (Fig. 2*B*), indicating that TBPB is not acting at a site identical to the orthosteric binding site.

To further evaluate the effects of TBPB at the orthosteric binding site of $M_1$, we evaluated the effects of TBPB on activation of $M_1$ in the presence of increasing concentrations of the nonselective orthosteric mAChR antagonist atropine. As seen in Figure 3*A*, increasing concentrations of atropine (1–10 nM) competitively antagonized the action of the orthosteric agonist CCh at the $M_1$ receptor. In contrast, increasing concentrations of atropine (0.3–3.0 nM) produced a robust decrease in the maximum effect of TBPB at $M_1$, consistent with a noncompetitive interaction (Fig. 3*B*). Together, the finding that a competitive orthosteric antagonist blocks the effect of TBPB in a noncompetitive manner along with the lack of effect of the mutation of the orthosteric site on TBPB action provides strong support for the hypothesis that TBPB is an allosteric agonist.

Although recent studies have attempted to develop $M_1$-selective orthosteric agonists, these compounds fail to exhibit true subtype selectivity attributable to the high conservation of the ACh binding site across the five mAChR subtypes. However, allosteric modulators often provide unprecedented selectivity relative to traditional orthosteric ligands. To determine whether TBPB exhibits selectivity for $M_1$ relative to $M_2$–$M_5$, we deter-

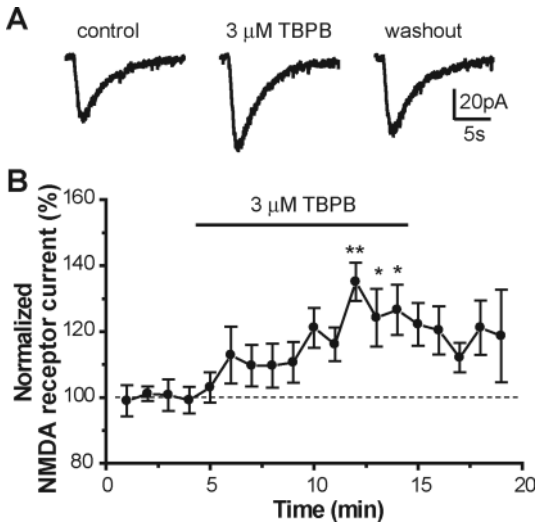


**Figure 6.** TBPB potentiates NMDA receptor currents in CA1 pyramidal cells. ***A***, Representative traces of NMDA-evoked currents obtained before TBPB application (control), at the peak of TBPB-induced potentiation (3 $\mu$M TBPB) and after washout of TBPB. ***B***, Time course studies reveal a slow development of TBPB-induced potentiation of NMDA receptor currents (*$p < 0.05$; **$p < 0.01$).

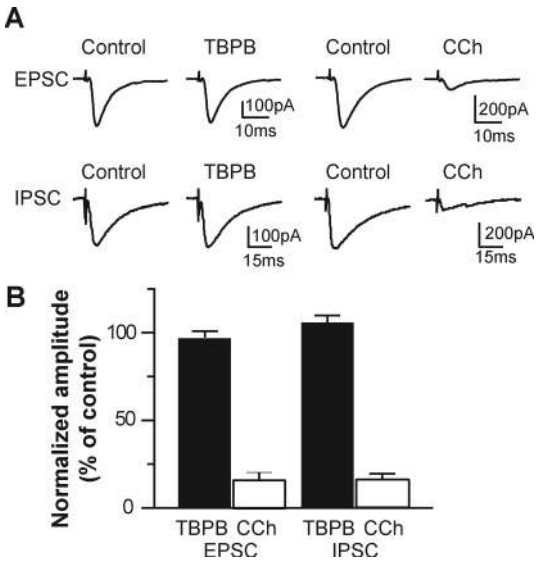


**Figure 7.** TBPB had no effects on evoked EPSCs and IPSCs in CA1 hippocampal pyramidal cells. ***A***, Average traces of EPSCs or IPSCs before application of TBPB or CCh (control), during application of TBPB (10 $\mu$M for EPSCs; 3 $\mu$M for IPSCs) or CCh (100 $\mu$M) from four different cells. TBPB had no effect on the amplitudes of evoked EPSCs (97.4 $\pm$ 4.0% of control; $n = 5$; $p > 0.5$) or IPSCs (106.5 $\pm$ 3.3% of control; $n = 4$; $p > 0.1$, Wilcoxon's matched-pair test) in hippocampal pyramidal cells. In parallel studies, CCh induced robust inhibition of EPSC and IPSC amplitudes (16.5 $\pm$ 4.0% of control, $n = 5$ and 15.4 $\pm$ 3.1%, $n = 5$, respectively; Wilcoxon's matched-pair test). ***B***, Bar graph summarizes the effect of TBPB or CCh on EPSC and IPSC amplitude. All data represent mean $\pm$ SEM of five to six cells.

mined effects of this compound on all members of the mAChR subfamily. For comparison, we also determined the effects of one of the more recently developed orthosteric agonists, AF267B, which has been purported to provide greater selectivity than previous orthosteric mAChR agonists (Caccamo et al., 2006). The effects of AF267B and TBPB were determined in cell lines expressing $rM_1$, $hM_2$–$G_{qi5}$, $hM_3$, $rM_4$–$G_{qi5}$, or $hM_5$. Although AF267B did provide greater selectivity than most other orthosteric agonists, these studies revealed that this compound lacks true selectivity and has robust agonist activity at $M_1$, $M_3$, and $M_5$ receptors (Fig. 4*A*). In contrast, TBPB was highly selective for $M_1$ and had no agonist activity at any of the other mAChR subtypes ($M_2$–$M_5$) at concentrations up to 10 $\mu$M (Fig. 4*B*).

### TBPB increases non-amyloidogenic APP processing

One of the most exciting effects of AF267B reported in previous studies was the finding that this compound has actions that may produce disease-modifying effects in AD. Thus, this compound decreased amyloidogenic processing of the APP and decreased development of amyloid pathology in 3xTg–AD mice (Caccamo et al., 2006). Although this finding was postulated to be mediated by $M_1$, the lack of selectivity of AF267B made it impossible to determine whether selective activation of $M_1$ would have a beneficial effect on APP processing. Thus, to clarify the potential role of $M_1$ in modulation of amyloid pathology, we investigated the effects of TBPB on the processing of the APP *in vitro* in PC12 cells.

A$\beta$ peptide is generated by the proteolysis of APP, which can be processed through either an amyloidogenic or non-amyloidogenic pathway. In the amyloidogenic pathway, APP is sequentially cleaved by $\beta$-secretase and then $\gamma$-secretase, resulting in the release of the A$\beta$ peptide. In the non-amyloidogenic pathway, APP is cleaved within the A$\beta$ domain by $\alpha$-secretase, releasing $APP_{s\alpha}$ and precluding the generation of A$\beta$ (Hardy et al., 2002). In the present study, PC12 cells overexpressing human sequence APP and $M_1$ were treated with vehicle, CCh, or TBPB, and the conditioned media were analyzed for APP derivatives. Treatment with 1 $\mu$M TBPB increased the shedding of $APP_{s\alpha}$, the ectodomain released by $\alpha$-secretase cleavage, by 58% compared with vehicle-treated cells (Fig. 5*A*,*B*). The magnitude of the TBPB response was comparable with that of the CCh-positive control and was blocked by atropine. It should be noted that the antibody used to detect $APP_s$ in these experiments recognizes an epitope contained within $APP_{s\alpha}$ but not $APP_{s\beta}$, indicating that the shedding of $APP_{s\alpha}$ is specifically increased. Consistent with these data, TBPB also increased the production of CTF$\alpha$ (also called C83), the C-terminal fragment of APP derived from $\alpha$-secretase cleavage, in an atropine-sensitive manner (Fig. 5*A*,*C*). We also analyzed conditioned media from these cells for A$\beta_{40}$ by ELISA (Fig. 5*D*). In TBPB-treated cells, A$\beta_{40}$ levels were reduced to 61% of the vehicle control, and this effect was blocked by atropine. Together, these results are consistent with the hypothesis that selective activation of $M_1$ could regulate APP processing and indicate that activation of $M_1$ with TBPB shifts the processing of APP toward the non-amyloidogenic pathway, resulting in increased shedding of $APP_{s\alpha}$ and decreased production of A$\beta$.

### TBPB potentiates NMDA receptor currents in CA1 hippocampal pyramidal cells

A prominent effect of activation of mAChRs in the hippocampus and other brain regions is potentiation of currents through the NMDA subtype of the glutamate receptor. Potentiation of NMDAR currents is thought to be important for both cognition and psychosis and has been postulated to play a role in the antipsychotic effects of mAChR agonists (Coyle et al., 2002; Marino et al., 2002). Previous studies suggest that potentiation of NMDAR currents in hippocampal pyramidal cells by nonselective mAChR agonists is mediated by $M_1$ (Marino et al., 1998). In contrast, presynaptic mAChRs involved in regulating synaptic transmission are not likely to involve $M_1$ activation. We showed recently that mAChR inhibition of EPSCs at the Schaffer collat-

eral–CA1 synapse is likely mediated by $M_4$ (Shirey et al., 2008), and $M_2$ has been postulated to play a major role in inhibiting transmission at inhibitory synapses in the hippocampus (Rouse et al., 1999). Given the possible importance of potentiation of NMDAR currents to the antipsychotic effects of mAChR agonists, it is important to determine whether TBPB mimics this effect of less selective mAChR agonists. If TBPB acts as an $M_1$ agonist in native systems and retains its selectivity for $M_1$ relative to other mAChR subtypes, then it should potentiate NMDAR currents but may have no effect on either inhibitory or excitatory synaptic transmission. Thus, we determined the effects of TBPB in hippocampal pyramidal cells using whole-cell patch-clamp recording techniques. Pressure ejection of NMDA (0.5 mM) produced a stable inward current in CA1 pyramidal cells voltage clamped at −60 mV. Bath application of TBPB (3 μM) produced an increase in the peak amplitude of NMDA-evoked currents in CA1 pyramidal cells (Fig. 6*A*,*B*). The increased amplitude of NMDAR currents induced by TBPB peaked at 135.1 ± 5.8% of baseline ~8 min after initial application of TBPB ($n = 6$). To confirm that the observed effects of TBPB were mediated by activation of mAChRs, the muscarinic antagonist atropine was applied to the bath before TBPB application. Atropine (1 μM) completely blocked the ability of TBPB (3 μM) to potentiate NMDA-evoked currents with a peak potentiation of TBPB-mediated effects of 5.1 ± 5.8% in combination with atropine ($n = 5$) compared with a peak potentiation of 40.4 ± 6.4% observed with TBPB alone ($p < 0.003$) (data not shown). In contrast, TBPB had no effect on the amplitudes of evoked EPSCs or IPSCs in hippocampal pyramidal cells (Fig. 7). Activation of mAChRs with CCh induced robust inhibition of both EPSC and IPSC amplitudes, indicating that the previously reported mAChR regulation of inhibitory and excitatory synaptic transmission in these cells was intact (Fig. 7*A*,*B*).

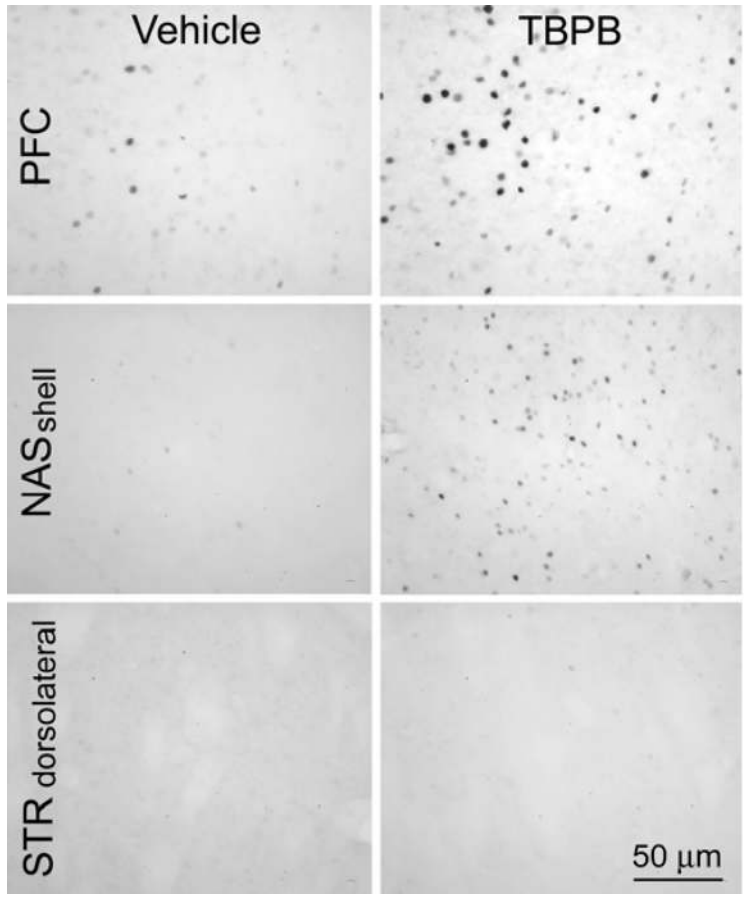


**Figure 8.** TBPB elicits Fos expression in the rat forebrain. Representative photomicrographs illustrate that TBPB (100 mg/kg) induces Fos-like immunoreactivity in the PFC and shell region of the nucleus accumbens ($NAS_{shell}$) but not in the dorsolateral striatum ($STR_{dorsolateral}$). Scale bar, 50 μm

**Table 1. The effects of TBPB on induction of Fos expression in rat brain regions**

| | Number of Fos-li cells/mm$^2$ | |
|---|---|---|
| Brain region | Vehicle | TBPB |
| PFC | 94.1 ± 17.9 | 326.3 ± 57.1* |
| NAS shell | 8.3 ± 2.8 | 72.2 ± 12.6** |
| NAS core | 1.9 ± 0.9 | 40.3 ± 13.4* |
| DStr lateral | 0.5 ± 0.5 | 2.3 ± 1.3 |
| DStr medial | 0.9 ± 0.6 | 4.2 ± 1.2* |

The effect of TBPB (100 mg/kg, s.c.) or vehicle treatment on induction of Fos expression were evaluated in the following rat brain regions: prefrontal cortex (PFC), shell region of the nucleus accumbens (NAS shell), core region of the nucleus accumbens (NAS core), lateral region of the dorsal striatum (DStr lateral), and medial region of the dorsal striatum (DStr medial). Data represent the mean ± SEM number of Fos-like immunoreactive neurons per square millimeter for six rats per treatment group, vehicle, or a subcutaneous dose of 100 mg/kg TBPB, in each region. Data were analyzed using a Student's *t* test comparison. *$p < 0.05$; **$p < 0.01$.

**TBPB produces antipsychotic-like effects in rodent models predictive of antipsychotic-like activity**

Discovery of a highly selective allosteric agonist of $M_1$ with activity in native systems provides a novel tool to allow us to determine whether a selective agonist of $M_1$ can mimic the effects of the $M_1/M_4$-preferring mAChR agonist xanomeline in animal models used to predict potential antipsychotic-like activity, including changes in Fos-li that are known to be characteristic of marketed antipsychotic agents and reversal of psychostimulant-induced behaviors.

Previous studies have demonstrated that a range of antipsychotic drugs induce changes in Fos-li in specific brain nuclei thought to be related to their clinical efficacy (for review, see Deutch et al., 1994; Fibiger et al., 1994). In particular, clozapine and other atypical antipsychotics induce preferential increases in Fos-li in the NAS and PFC but not in the dorsolateral STR, whereas typical antipsychotics, such as the selective $D_2$ dopamine receptor antagonist haloperidol, increase Fos expression in the STR and NAS but not the PFC. Interestingly, the pattern of Fos-li induced by the mAChR agonist xanomeline is virtually identical to that induced by atypical antipsychotics (Perry et al., 2001). However, the specific mAChR subtype responsible for this effect of xanomeline is not known. Here we evaluated the ability of TBPB to induce Fos-li in three rat brain regions, specifically the PFC, NAS, and STR. TBPB (100 mg/kg, s.c.) selectively increased the number of Fos-li cells in both the PFC ($t_{(10)} = 3.88$; $p < 0.01$) and NAS (shell, $t_{(10)} = 4.94$, $p < 0.001$; and core, $t_{(10)} = 1.32$, $p > 0.05$) but not in the dorsolateral STR (Fig. 8, Table 1). These effects of TBPB on Fos expression indicate that selective activation of $M_1$ receptors is sufficient to induce changes in Fos-li comparable with previously reported effects of xanomeline.

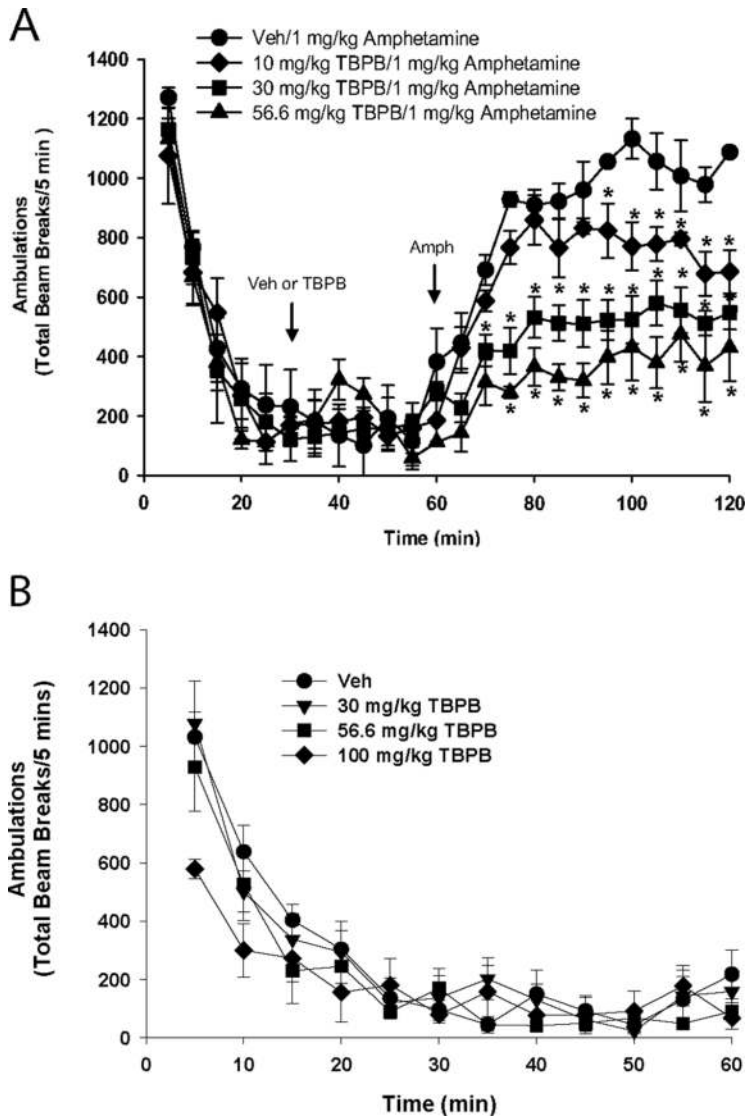


**Figure 9.** TBPB produces a robust inhibition of amphetamine-induced hyperlocomotion. ***A***, TBPB produces a dose-dependent decrease in amphetamine-induced hyperlocomotion. ***B***, TBPB does not impair motor output at doses that produce antipsychotic-like activity. Data are expressed as mean ± SEM of the number of beam breaks/5 min. SEM are not shown if less than the size of the point ($n = 6–8$ per dose). *$p < 0.05$ vs vehicle plus amphetamine (1.0 mg/kg), Dunnett's test. Veh, Vehicle; Amph, amphetamine.

Both typical and atypical antipsychotic drugs reduce amphetamine-induced hyperlocomotion, an effect thought to be predictive of their antipsychotic efficacy (for review, see Geyer et al., 2003). As with changes in Fos expression, xanomeline also exhibits effects in preclinical models comparable with those observed with the atypical antipsychotic clozapine. Again, this effect is likely to be relevant for the clinical efficacy of xanomeline in schizophrenia patients, but the mAChR subtypes involved in mediating this effect are unclear. Thus, we determined whether selective activation of $M_1$ by TBPB could mimic the effects of antipsychotics and xanomeline in reversing amphetamine-induced hyperlocomotion in rats. TBPB produced a robust, dose-related inhibition of amphetamine-induced hyperlocomotion, which was significant after subcutaneous doses of 10, 30, and 56.6 mg/kg (Fig. 9*A*). TBPB had no effect on general locomotor output across the dose range tested (30–100 mg/kg, s.c.) when administered alone (Fig. 9*B*).

### TBPB produces antipsychotic-like effects at doses that do not produce catalepsy or side effects associated with activation of peripheral $M_2$ and $M_3$ mAChRs

Typical antipsychotics, such as the selective $D_2$ dopamine receptor antagonist haloperidol, are associated with dose-limiting motor impairments clinically attributable to excessive antagonism of $D_2$ dopamine receptors (Reynolds et al., 2004). A potential advantage of $M_1$ agonists could be the ability to produce efficacy in schizophrenia patients without inducing the adverse motor effects of existing antipsychotic therapies. Thus, we evaluated the ability of TBPB to produce catalepsy, a preclinical model of motor impairment. TBPB (30–100 mg/kg, s.c.) did not induce catalepsy up to 4 h (Fig. 10*A*, left). Our data with TBPB are consistent with the lack of catalepsy observed with xanomeline (Shannon et al., 2000). Similarly, clozapine also failed to produce catalepsy (Fig. 10*A*, right). In contrast, haloperidol produced dose- and time-related increases in catalepsy (Fig. 10*A*, middle). Thus, TBPB produced antipsychotic-like effects over a dose range that did not produce catalepsy. Our data suggest that TBPB does not produce robust functional antagonism of striatal dopaminergic function over the dose range tested and that selective activation of the $M_1$ mAChR may provide a novel antipsychotic approach without potential dose-limiting side effects, including the induction of extrapyramidal side effects.

Clinical studies using direct acting mAChR agonists, including xanomeline, and cholinesterase inhibitors have reported substantial dose-limiting adverse effects attributable to nonspecific activation of the mAChR subtypes, most notably peripheral $M_2$ and $M_3$ (Bodick, 1997a,b; Felder, 2001). Although TBPB is highly selective for the $M_1$ relative to the other mAChRs *in vitro*, it was important to evaluate the degree of selectivity of the actions of TBPB *in vivo*. Thus, the potential of TBPB to produce peripheral $M_2$- and $M_3$-mediated effects, including salivation, lacrimation, diarrhea, and changes in respiratory rate, was assessed using a modified Irwin neurological test battery with the nonselective mAChR agonist oxotremorine as a comparator. Oxotremorine produced a robust dose-dependent induction of salivation (Fig. 10*B*). In contrast, TBPB did not produce any salivation across the dose range of 30–100 mg/kg (Fig. 10*B*). In addition, oxotremorine produced a dose-dependent induction of lacrimation, diarrhea, piloerection, and decreased respiratory rate and core body temperature, whereas TBPB did not produce these effects, with the exception of a slight decrease in core body temperature at 100 mg/kg (data not shown). Thus, TBPB produced antipsychotic-like activity at doses that did not produce adverse effects associated with activation of peripheral $M_2$ and $M_3$ mAChRs *in vivo*.

### TBPB does not occupy central $D_2$ dopamine receptors at doses that produce antipsychotic-like effects

Our initial *in vivo* characterization of TBPB indicates a profile of effects in preclinical models predictive of antipsychotic-like activity similar to those observed with xanomeline and the atypical antipsychotic clozapine. Because the antipsychotic effects of currently marketed antipsychotic agents is thought to involve antagonism of $D_2$ dopamine receptors (Reynolds et al., 2004), we evaluated the affinity of TBPB at $D_2$ receptors using the National Institute of Mental Health Psychoactive Drug Screening Program (http://pdsp.med.unc.edu/, accession number 3156). TBPB had relatively low affinity for $D_2$ ($K_i$ of 1.4 $\mu$M) receptors. Although this affinity is significantly lower than the potency of TBPB at activating $M_1$, it is well established that antagonism of $D_2$ dopamine receptors can produce antipsychotic-like effects in animal models similar to the effects observed with TBPB (for review, see Geyer et al., 2003). The present studies of the effects of TBPB on Fos-li and measures of catalepsy suggest that TBPB does not act by blockade of $D_2$. However, to definitively assess the possibility that the doses of TBPB used in these studies occupy $D_2$ dopamine receptors, we determined the occupancy of central $D_2$ dopamine receptors by TBPB. $D_2$ occupancy was evaluated by measuring displacement of [$^{18}$F]fallypride, a high-affinity dopamine $D_2$ receptor radioligand, using positron emission tomography. This radioligand has been used in several studies for the evaluation of $D_2$ receptor occupancy by various antipsychotic drugs, including clozapine, risperidone, and haloperidol, in rodents, nonhuman primates, and humans (Mukherjee et al., 2001; Kessler et al., 2005, 2006). As a positive control, we also determined the occupancy by haloperidol of central $D_2$ receptors after doses of 0.1 and 1.0 mg/kg, doses that produce moderate to full reversal of amphetamine-induced hyperlocomotion (Stanhope et al., 2001). Using a within-subject design, control binding potentials of [$^{18}$F]fallypride were first assessed after vehicle alone, followed 1 week later by measurement of binding potentials of [$^{18}$F]fallypride in the presence of a dose of TBPB or haloperidol. Changes in binding potential of [$^{18}$F]fallypride for $D_2$ in rat striatum (caudate–putamen), a region with high $D_2$ dopamine receptor expression levels, were calculated from distribution volume ratio estimates using a Logan plot (Logan et al., 1996; Mukherjee et al., 2001). TBPB produced no change in the binding potential of [$^{18}$F]fallypride in rat striatum (Fig. 11*D*) compared with vehicle treatment (Fig. 11*A*). In contrast, haloperidol produced a robust dose-related decrease in the binding potentials of [$^{18}$F]fallypride in rat striatum after treatment with 0.1 (Fig. 11*E*) and 1.0 mg/kg (Fig. 11*F*) of haloperidol compared with the vehicle treatment (Table 2, Fig. 11*B*,C). These findings indicate that TBPB does not occupy $D_2$ receptors at doses that produce antipsychotic-like effects *in vivo*.

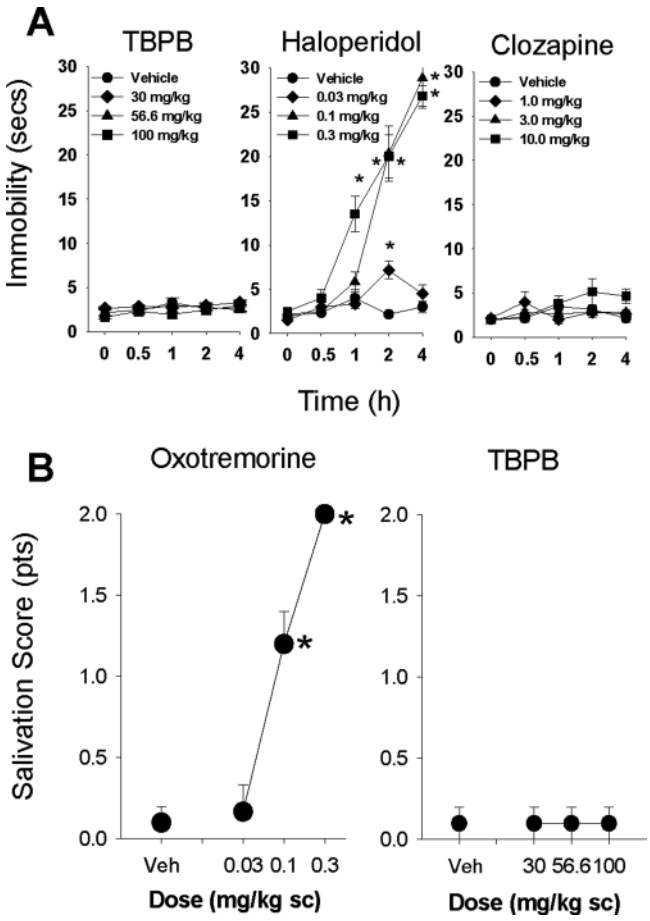


**Figure 10.** TBPB produces antipsychotic-like effects at doses that do not produce catalepsy or induction of salivation. ***A***, Dose- and time-related cataleptic immobility produced by haloperidol (middle) and lack of cataleptic immobility produced by TBPB (left) and clozapine (right) in rats. Haloperiodol produced catalepsy; significant after subcutaneous dose of 0.1 and 0.3 mg/kg by a Dunnett's comparison with the vehicle group. ***B***, Dose-related induction of salivation produced by oxotremorine (left) and the lack of salivation produced by TBPB (right). Oxotremorine produced a robust dose-dependent induction of salivation, significant after subcutaneous dose of 0.1 and 0.3 mg/kg by a Dunnett's comparison with the vehicle (Veh) group. Results are expressed as mean ± SEM ($n = 6$ per treatment group). *$p < 0.05$ when compared with the vehicle control group.

## Discussion

Discovery and characterization of TBPB as a highly selective allosteric agonist of the $M_1$ mAChR provides a major advance in further demonstrating the feasibility of achieving high selectivity for $M_1$ mAChRs by targeting allosteric sites. These studies provide exciting new data revealing that selective activation of $M_1$ provides efficacy in animal models that predict antipsychotic efficacy and that are responsive to the $M_1$/$M_4$-preferring mAChR agonist xanomeline, which has demonstrated antipsychotic efficacy in the clinic. In addition, the selective activation of $M_1$ by TBPB also results in enhanced processing of APP through the nonamyloidogenic pathway, which may constitute a potential disease modifying approach for AD. Based on a (1-(1′-substituted)-1,4′-bipiperidin-4-yl)-1*H*-benzo[*d*]imidazol-2(3*H*)-one scaffold, TBPB is structurally and chemically distinct from other mAChR agonists (Kinney et al., 2006) and provides higher selectivity for $M_1$ relative to other mAChR subtypes than xanomeline or other published orthosteric mAChR agonists.

Our findings provide strong evidence that the antipsychotic-like effects of xanomeline in animal models can be mimicked by selective activation of $M_1$ and raise the exciting possibility that selective allosteric activators of $M_1$ may provide antipsychotic efficacy in patients. Interestingly, we and others reported recently that *N*-desmethylclozapine, a major metabolite of the atypical antipsychotic clozapine, preferentially activates $M_1$ mAChRs (Sur et al., 2003; Weiner et al., 2004). Like TBPB, *N*-desmethylclozapine is an allosteric agonist of $M_1$ and fully activates the $M_1$ (Y381A) mutant (Sur et al., 2003). Interestingly, Weiner et al. (2004) found that the plasma levels of *N*-desmethylclozapine are more closely correlated with clinical response to clozapine than are plasma levels of the parent compound. Although this does not establish $M_1$ activation as contributing to the unique efficacy profile of clozapine, it does raise this possibility.

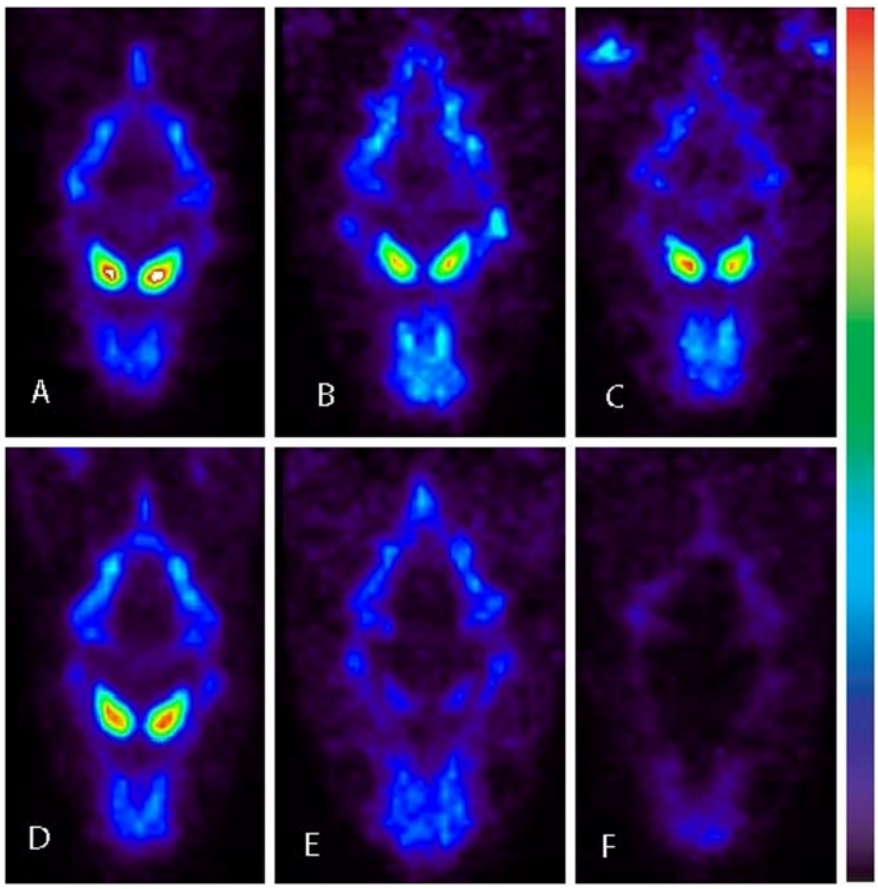


**Figure 11.** TBPB does not occupy central $D_2$ dopamine receptors at doses that produce antipsychotic-like effects. Representative PET images showing [$^{18}$F]fallypride binding in rat striatum after vehicle (***A–C***) or a dose of TBPB (100 mg/kg, s.c.) (***D***), haloperidol (0.1 mg/kg, s.c.) (***E***), or haloperidol (1.0 mg/kg s.c.) (***F***) pretreatment. Single slices of the images that were summed over the duration of the scans are depicted. The slice thickness is 0.08 cm.

**Table 2. TBPB does not occupy central $D_2$ dopamine receptors at a dose that produces antipsychotic activity *in vivo***

| Drug treatment (mg/kg) | Control binding potential | Postdrug binding potential | $D_2$ dopamine receptor occupancy |
|---|---|---|---|
| TBPB (100) | 14.2 (3.5) | 14.6 (2.8) | −2.8% |
| Haloperidol (0.1) | 14.6 (3.3) | 4.2 (0.5) | 71.2% |
| Haloperidol (1.0) | 13.7 (1.4) | 1.4 (0.3) | 89.8% |

Rat numbers used for the TBPB study and each of the haloperidol studies were 7, 3, and 3, respectively. Data represent the calculated control binding potential of [$^{18}$F]Fallypride alone or after treatment with subcutaneous does of 100 mg/kg TBPB or subcutaneous dose of 0.1 or 1.0 mg/kg haloperidol in rat striatum (means ± SE; binding potential = Logan DVR − 1). The Logan DVR values of each study were obtained by using cerebellum as the reference tissue. Percentage $D_2$ dopamine receptor occupancy was calculated as $(1 - [\text{binding potential}_{drug}/\text{binding potential}_{control}]) \times 100$.

Although the present studies point to $M_1$ as a major contributor to the effects of muscarinic agonists in the models predictive of antipsychotic activity, it is important to mention that these data do not rule out a possible role for $M_4$. As discussed above, xanomeline has similar potencies as an agonist of $M_1$ and $M_4$. Recent findings with both $M_1$ and $M_4$ knock-out mice support possible roles for each of these receptor subtypes (Gerber et al., 2001; Zhang et al., 2002; Anagnostaras et al., 2003) in the effects observed with xanomeline. For example, Zhang et al. (2002) reported that oxotremorine-stimulated release of striatal [$^3$H]dopamine was totally abolished in $M_4$ mAChR knock-out mice, indicating that $M_4$ receptors play a key role in promoting mAChR-dependent increases in striatal dopamine output. Thus, in future studies, it will be critical to further evaluate the relative effects of agents that are selective for $M_1$ and $M_4$, as well as combined administration of $M_1$ and $M_4$ agonists in animal models that predict antipsychotic efficacy, negative symptoms, and relevant aspects of cognitive function.

The mechanisms by which selective activation of $M_1$ may have antipsychotic efficacy are not entirely clear. However, one possible mechanism that could contribute to the effects of TBPB may be through the potentiation of NMDAR currents in the hippocampus and other neocortical sites. Activation of NMDARs is critical in the regulation of hippocampal and cortical function and is thought to be important for the cognition-enhancing effects of mAChR activation. In addition, the NMDAR may play an important role in regulation of circuits that are disrupted in schizophrenia and other psychotic disorders (for review, see Coyle et al., 2002; Marino et al., 2002). Thus, a large number of clinical and animal studies have led to the hypothesis that potentiation of NMDAR currents in these regions could have an antipsychotic action. The present finding that selective activation of $M_1$ by TBPB potentiates NMDAR currents in CA1 hippocampal cells provides one possible mechanism by which selective allosteric $M_1$ mAChR agonists could have therapeutic utility in psychiatric and neurological disorders in which hippocampal or NMDAR function is thought to be compromised.

Our findings with TBPB also provide critical support for the hypothesis that $M_1$ activation has effects that could prove beneficial to patients suffering from AD. AD is the most common neurodegenerative disorder in elderly populations, affecting eight million people worldwide, resulting in progressive memory loss and severe cognitive dysfunction attributable in large part to the impaired function of the forebrain cholinergic system (Sorbera et al., 2007). Clinical studies using both direct- and indirect-acting muscarinic agonists have reported improvements in the behavioral disturbances associated with AD (Bodick et al., 1997; Cummings et al., 2001), although dose-limiting side effects resulting from the activation of peripheral mAChRs have rendered these nonselective mAChR agonists unsuitable for clinical treatment. Moreover, the muscarinic agonist AF102B [(2*R*,3*R*)2-methyl-spiro[1-azabicyclo[2.2.2]octane-3,5′-[1,3]oxathiolane], an analog of AF267B [(*S*)-2-ethyl-8-methyl-1-thia-4,8-diazaspiro[4.5]decan-3-one], decreased the production of the amyloidogenic peptide $A\beta_{42}$ in the CSF of AD patients, suggesting that mAChR activation may have potential to be disease modifying as well as providing palliative cognitive therapy (Eglen et al., 1999; Tarsy et al., 2006). Preclinical studies with AF267B in 3xTg–AD mice provide additional support for a disease-modifying role of mAChR activation (Caccamo et al., 2006). However, because AF267B is a relatively nonselective muscarinic agonist as demonstrated in the

present study, it has been difficult to confirm which of the mAChR subtypes are most important in mediating these AD-modifying effects. Selective activation of $M_1$ by TBPB increases non-amyloidogenic processing and reduces A$\beta$ formation, as reported previously with other nonselective muscarinic agonists. These data are consistent with the hypothesis that the effects of AF267B on APP processing are mediated by $M_1$ and provide evidence that selective $M_1$ activation by an allosteric mechanism may provide a novel disease-modifying approach for AD. In future studies, it will be important to perform additional *in vivo* studies with TBPB in 3xTg–AD mice to determine whether the range of effects of AF267B in these animals can be induced by the more selective $M_1$ agonist. Also, it will be important to determine effects of TBPB in other AD models and animal models of cognitive function.

In summary, TBPB is a highly selective, allosteric agonist of the $M_1$ mAChR with robust efficacy in potentiating NMDAR currents, processing of APP through the non-amyloidogenic pathway, and in preclinical models predictive of antipsychotic-like activity. Our findings confirm and extend the role of the $M_1$ mAChR in many of the documented effects of the $M_1/M_4$-preferring muscarinic orthosteric agonist xanomeline. Moreover, the present data indicate that selective activation of $M_1$ may provide a novel therapeutic approach for the treatment of psychotic symptoms associated with schizophrenia and AD.

## References


Anagnostaras SG, Murphy GG, Hamilton SE, Mitchell SL, Rahnama NP, Nathanson NM, Silva AJ (2003) Selective cognitive dysfunction in acetylcholine M1 muscarinic receptor mutant mice. Nat Neurosci 6:51–58.

Ansari MS, Kessler RM, Clanton JA, de Paulis T, Baldwin RM (2006) Comparison of three [$^{18}$F]fallypride methods intended for automated remote chemistry modules. J Nucl Med 47:159P.

Bodick NC, Offen WW, Levey AI, Cutler NR, Gauthier SG, Satlin A, Shannon HE, Tollefson GD, Rasmussen K, Bymaster FP, Hurley DJ, Potter WZ, Paul SM (1997a) Effects of xanomeline, a selective muscarinic receptor agonist, on cognitive function and behavioral symptoms in Alzheimer disease. Arch Neurol 54:465–473.

Bodick NC, Offen WW, Shannon HE, Satterwhite J, Lucas R, van Lier R, Paul SM (1997b) The selective muscarinic agonist xanomeline improves both the cognitive deficits and behavioral symptoms of Alzheimer disease. Alzheimer Dis Assoc Disord 11 [Suppl 4]:S16–S22.

Bonner TI, Buckley NJ, Young AC, Brann MR (1987) Identification of a family of muscarinic acetylcholine receptor genes. Science 237:527–532.

Bonner TI, Young AC, Brann MR, Buckley NJ (1988) Cloning and expression of the human and rat m5 muscarinic acetylcholine receptor genes. Neuron 1:403–410.

Bubser M, Deutch AY (2002) Differential effects of typical and atypical antipsychotic drugs on striosome and matrix compartments of the striatum. Eur J Neurosci 15:713–720.

Bymaster FP, Carter PA, Peters SC, Zhang W, Ward JS, Mitch CH, Calligaro DO, Whitesitt CA, DeLapp N, Shannon HE, Rimvall K, Jeppesen L, Sheardown MJ, Fink-Jensen A, Sauerberg P (1998) Xanomeline compared to other muscarinic agents on stimulation of phosphoinositide hydrolysis *in vivo* and other cholinomimetic effects. Brain Res 795:179–190.

Caccamo A, Oddo S, Billings LM, Green KN, Martinez-Coria H, Fisher A, LaFerla FM (2006) M1 receptors play a cnetral role in modulating AD-like pathology in transgenic mice. Neuron 49:671–682.

Christopoulos A (2002) Allosteric binding sites on cell-surface receptors: novel targets for drug discovery. Nat Rev Drug Discov 1:198–210.

Coyle JT, Tsai G, Goff DC (2002) Ionotropic glutamate receptors as therapeutic targets in schizophrenia. Curr Drug Target CNS Neurol Disord 1:183–189.

Cummings JL, Nadel A, Masterman D, Cyrus PA (2001) Efficacy of metrifonate in improving the psychiatric and behavioral disturbances of patients with Alzheimer's disease. J Geriatr Psychiatry Neurol 14:101–108.

Deutch AY (1994) Identification of the neural systems subserving the actions of clozapine: clues from immediate-early gene expression. J Clin Psychiatry 55 [Suppl B]:37–42.

Eglen RM, Choppin A, Watson N (2001) Therapeutic opportunities from muscarinic research. Trends Pharmacol Sci 22:409–414.

Felder CC, Porter AC, Skillman TL, Zhang L, Bymaster FP, Nathanson NM, Hamilton SE, Gomeza J, Wess J, McKinzie DL (2001) Elucidating the role of muscarinic receptors in psychosis. Life Sci 68:2605–2613.

Fibiger HC (1994) Neuroanatomical targets of neuroleptic drugs as revealed by Fos immunochemistry. J Clin Psychiatry 55 [Suppl B]:33–36.

Gerber DJ, Sotnikova TD, Gainetdinov RR, Huang SY, Caron MG, Tonegawa S (2001) Hyperactivity, elevated dopaminergic transmission, and response to amphetamine in M1 muscarinic acetylcholine receptor-deficient mice. Proc Natl Acad Sci U S A 98:15312–15317.

Geyer MA, Ellenbroek B (2003) Animal behavior models of the mechanisms underlying antipsychotic atypicality. Prog Neuropsychopharmacol Biol Psychiatry 7:1071–1107.

Hardy J, Selkoe DJ (2002) The amyloid hypothesis of Alzheimer's disease: progress and problems on the road to therapeutics. Science 297:353–356.

Hemstapat K, Da Costa H, Nong Y, Brady AE, Luo Q, Niswender CM, Tamagnan GD, Conn PJ (2007) A novel family of potent negative allosteric modulators of group II metabotropic glutamate receptors. J Pharmacol Exp Ther 322:254–264.

Irwin S (1968) Comprehensive observational assessment: IA. A systematic, quantitative procedure for assessing the behavioral and physiologic state of the mouse. Psychopharmacologia 13:222–257.

Jones CK, Brady AE, Bubser M, Deutch AY, Williams LC et al (2006) TBPB is a highly selective M1 allosteric muscarinic receptor agonist *in vitro* and produces robust antipsychotic-like effects *in vivo*. Neuropsychopharmacology 31:S116.

Kessler RM, Votaw JR, de Paulis T, Bingham DR, Ansari MS, Mason NS, Holburn G, Schmidt DE, Votaw DB, Manning RG, Ebert MH (1993) Evaluation of 5-[$^{18}$F]fluoropropylepidepride as a potential PET radioligand for imaging dopamine $D_2$ receptors. Synapse 15:169–176.

Kessler RM, Ansari MS, Riccardi P, Li R, Jayathilake K, et al (2005) Occupancy of striatal and extrastriatal dopamine D2/D3 receptors by olanzapine and haloperidol. Neuropsychopharmacology 30:2283–2289.

Kessler RM, Ansari MS, Riccardi P, Li R, Jayathilake K, Dawant B, Meltzer HY (2006) Occupancy of striatal and extrastriatal dopamine D2 receptors by clozapine and quetiapine. Neuropsychopharmacology 31:1991–2001.

Kinney GG (2006) Muscarinic receptor activation for the treatment of schizophrenia. Neuropsychopharmacology 31:S26.

Levey AI, Kitt CA, Simonds WF, Price DL, Brann MR (1991) Identification and localization of muscarinic acetylcholine receptor proteins in brain with subtype-specific antibodies. J Neurosci 11:3218–3226.

Logan J, Fowler JS, Volkow ND, Wang GJ, Ding YS, Alexoff DL (1996) Distribution volume ratios without blood sampling from graphical analysis and PET data. J Cereb Blood Flow Metab 16:834–840.

Marino MJ, Conn PJ (2002) Direct and indirect modulation of the *N*-methyl D-aspartate receptor. Curr Drug Target CNS Neurol Disord 1:1–16.

Marino MJ, Rouse ST, Levey AI, Potter LT, Conn PJ (1998) Activation of the genetically defined m1 muscarinic receptor potentiates *N*-methyl-D-aspartate (NMDA) receptor currents in hippocampal pyramidal cells. Proc Natl Acad Sci U S A 95:11465–11470.

Moore NA, Tye NC, Axton MS, Risius FC (1992) The behavioral pharmacology of olanzapine, a novel "atypical" antipsychotic agent. J Pharmacol Exp Ther 262:545–551.

Mukherjee J, Christian BT, Narayanan TK Shi B, Mantil J (2001) Evaluation of dopamine D-2 receptor occupancy by clozapine, risperidone, and haloperidol *in vivo* in the rodent and nonhuman primate brain using 18F-fallypride. Neuropsychopharmacology 25:476–488.

Perry KW, Nisenbaum LK, George CA, Shannon HE, Felder CC, Bymaster FP (2001) The muscarinic agonist xanomeline increases monoamine release and immediate early gene expression in the rat prefrontal cortex. Biol Psychiatry 49:716–725.

Reynolds GP (2004) Receptor mechanisms in the treatment of schizophrenia. J Psychopharmacol 18:340–345.

Rodriguez AL, Nong Y, Sekaran NK, Alagille D, Tamagnan GD, Conn PJ (2005) A close structural analog of 2-methyl-6-(phenylethynyl)-pyridine acts as a neutral allosteric site ligand on metabotropic glutamate receptor subtype 5 and blocks the effects of multiple allosteric modulators. Mol Pharmacol 68:1793–1802.

Rouse ST, Marino MJ, Potter LT, Conn PJ, Levey AI (1999) Muscarinic receptor subtypes involved in hippocampal circuits. Life Sci 64:501–509.

Shannon HE, Rasmussen K, Bymaster FP, Hart JC, Peters SC, Swedberg MD,

Jeppesen L, Sheardown MJ, Sauerberg P, Fink-Jensen A (2000) Xanomeline, an M(1)/M(4) preferring muscarinic cholinergic receptor agonist, produces antipsychotic-like activity in rats and mice. Schizophr Res 42:249–259.

Shekhar A, Potter WZ, Lightfoot J, Lienemann J, Dubé S, Mallinckrodt C, Bymaster FP, McKinzie DL, Felder CC (2008) Selective muscarinic receptor agonist xanomeline as a novel treatment approach for schizophrenia. Am J Psychiatry 165:1033–1039.

Shirey JK, Xiang Z, Orton D, Brady AE, Johnson KA, Williams R, Ayala JE, Rodriguez AL, Wess J, Weaver D, Niswender CM, Conn PJ (2008) An allosteric potentiator of M4 mAChR modulates hippocampal synaptic transmission. Nat Chem Biol 4:42–50.

Spalding TA, Trotter C, Skjaerbaek N, Messier TL, Currier EA, Burstein ES, Li D, Hacksell U, Brann MR (2002) Discovery of an ectopic activation site on the M(1) muscarinic receptor. Mol Pharmacol 61:1297–1302.

Spalding TA, Ma JN, Ott TR, Friberg M, Bajpai A, Bradley SR, Davis RE, Brann MR, Burstein ES (2006) Structural requirements of transmembrane domain 3 for activation by the M1 muscarinic receptor agonists AC-42, AC-260584, clozapine, and *N*-desmethylclozapine: evidence for three distinct modes of receptor activation. Mol Pharmacol 70:1974–1983.

Sorbera LA, Bozzo J, Serradell N (2007) Alzheimer's disease one century later: the search for effective therapeutic targets continues. Drugs Future 32:625–641.

Stanhope KJ, Mirza NR, Bickerdike MJ, Bright JL, Harrington NR, Hesselink MB, Kennett GA, Lightowler S, Sheardown MJ, Syed R, Upton RL, Wadsworth G, Weiss SM, Wyatt A (2001) The muscarinic receptor agonist xanomeline has an antipsychotic-like profile in the rat. J Pharmacol Exp Ther 299:782–792.

Sur C, Mallorga PJ, Wittmann M, Jacobson MA, Pascarella D, Williams JB, Brandish PE, Pettibone DJ, Scolnick EM, Conn PJ (2003) *N*-Desmethylclozapine, a novel allosteric agonist at muscarinic 1 receptor potentiates *N*-methyl-D-aspartate receptor activity. Proc Natl Acad Sci U S A 100:13674–13679.

Tantawy MN, Peterson TE, Jones C, Baldwin RM, Ansari M, Kessler RM (2007) Feasibility of determining [$^{18}$F]Fallypride binding potential with delayed scans. Presented at the 54th Annual Meeting of the Society of Nuclear Medicine, Washington, DC, June 2–6.

Tarsy D, Simon DK (2006) Dystonia. N Engl J Med 335:818–829.

Waelbroeck M (2003) Allosteric drugs acting at muscarinic acetylcholine receptors. Neurochem Res 28:419–422.

Weiner DM, Meltzer HY, Veinbergs I, Donohue EM, Spalding TA, et al (2004) The role of M1 muscarinic receptor agonism of *N*-desmethylclozapine in the unique clinical effects of clozapine. Psychopharmacology 177:207–216.

Young CD, Bubser M, Meltzer HY, Deutch AY (1999) Clozapine pretreatment modifies haloperidol-elicited forebrain Fos induction: a regionally-specific double dissociation. Psychopharmacology 144:255–263.

Zhang W, Yamada M, Gomeza J, Basile AS, Wess J (2002) Multiple muscarinic acetylcholine receptor subtypes modulate striatal dopamine release, as studied with $M_1$–$M_5$ muscarinic receptor knock-out mice. J Neurosci 22:6347–6352.